Effect of the Ni/Co Ratio on the High-Temperature Oxidation Behavior of Ni&Co-Based 25Cr–0.4C–1.6Ti, wt%-Containing Cast Alloys

Patrice Berthod, Lydia Toubal

Effect of the Ni/Co ratio on the high temperature oxidation behavior of {Ni&Co}-based {25Cr-0.4C-1.6Ti, wt.%}-containing cast alloys

Patrice Berthod[1,2], Lydia Toubal[2]

[1]*Institut Jean Lamour (UMR CNRS 7198), Department CP2S,*
[2]*Faculty of Science and Technologies,*
University of Lorraine, Postal Box 70239, 54506 Vandoeuvre-lès-Nancy, FRANCE

patrice.berthod@centraliens-lille.org, lydia.toubal8@etu.univ-lorraine.fr

Abstract. Six alloys, based on Ni and/or Co with Co/(Ni+Co) ratio varying from 0 to 1, and containing 25wt.%Cr, 0.4wt.%C and 1.6wt.%Ti, were synthesized by conventional foundry way. Their as-cast microstructures were controlled by electron microscopy. Parts of these alloys, properly prepared on surface, were then exposed to atmospheric air during 20 hours at 1400K. The obtained surface states and sub-surfaces were characterized by optical observations and cross-sectional examinations by electron microscopy. The nickel-richest alloys contained more chromium carbides than titanium carbides while this was the opposite for the cobalt-richest alloys. This confirm the results of a recent study. It was furthermore found here that the alloys with many chromium carbides and few TiC were much better in oxidation at high temperature than the ones with many TiC and few chromium carbides. By considering the apparent involvement of titanium in the oxidation process it seems that the major influent parameter is directly the base element, independently on the nature of the obtained primary carbides.

Keywords: Nickel-based alloys; Cobalt-based alloys; Chromium carbides; Titanium carbides; High temperature oxidation

Post-print version of the article *Oxid Met (2018) 89:551–563; https://doi.org/10.1007/s11085-017-9808-3*

INTRODUCTION

Despite the supremacy of the γ/γ' single crystals the polycrystalline superalloys issued from classical foundry process keep great interest by allowing obtaining geometrically complex pieces for high temperature applications [1]. To be strong enough when used under stresses at elevated temperatures these alloys must be reinforced at the matrix level (e.g. by heavy atoms in solid solution or particles precipitation) as well as at the grain boundary level (e.g. by primary carbides). The most commonly used carbides for grain boundary strengthening are chromium carbides (containing, or not, other metallic elements) and the MC-type carbides. When the working temperature is higher than 1000°C, MC carbides must be preferred for their general better thermodynamic stability. Among the later ones, tantalum carbides are the most popular ones. TaC carbides are rather dense carbides (13.96g/cm^3 [2]), compared to TiC (4.85g/cm^3 [2]). With, in addition, a lower cost of Ti by comparison to Ta, using TiC instead TaC for the reinforcement of cast polycrystalline superalloys, appears to be envisaged.

Ti is a common element in superalloys [1], in which it may participate to the γ' composition [1] or complex MC carbides in association with other MC-forming metals (e.g. Haynes 282 superalloy [3]). It is also often present in alloys employed for medical applications [e.g. cobalt-titanium alloys [4, 5]. It was recently attempted to promote the formation of TiC carbides in chromia-forming quaternary cast alloys, based either on nickel [6] or on cobalt [7], by adding rather high quantities of Ti and of C with Ti/C atomic ratio equal to 1. TiC carbides were successfully obtained in the {Co-25wt.%Cr}-based alloys [7] in which they were almost the single carbides present. In contrast,

the {Ni-25wt.%Cr}-based alloys were almost free of TiC with the presence of chromium carbides only in their microstructures [6]. By substituting more or less nickel by cobalt in {M-25Cr-0.4C-1.6Ti}-type alloys (M=Ni and/or Co) one thought that it was maybe possible to obtain a greater fraction of the carbides being TiC. This was attempted [8] and, indeed it was observed that adding Co leads to an increasing part of TiC in the microstructure when the Co content increases. However, one can guess that the high temperature oxidation behavior of the Co-richest alloys of the series may be deteriorated. A study of the effect of an increasing part of cobalt in the alloys on their behavior in air at 1400K was then undertaken.

EXPERIMENTAL

The chemical compositions of the six alloys considered in this study are displayed in Table 1. All alloys contain 25wt.%Cr for their resistance against high temperature oxidation and corrosion, 0.4wt.%C to promote the formation of carbides in quantity high enough to significantly increase the mechanical resistance of the alloys at high temperature, and 1.6wt.%Ti to have as many titanium atoms as carbon atoms. After having subtracted to 100% the sum of the weight contents in Cr, Ti and C, one have shared in six proportions the rest between Ni and Co.

For each alloy, 40 grams of mix of pure metals (Alfa Aesar, purity higher than 99.9wt.%) were prepared and put in the copper crucible of the High Frequency induction furnace (CELES, France, 50kW). A silica tube was placed around the crucible to isolate the metallic parts from laboratory air. Pumping was performed out until reaching 5×10^{-2} mbars in the fusion chamber and 800mbars of pure argon was injected inside. These two operations were repeated three times. Heating and melting were realized in 300mbar of Ar, with about 2 minutes of heating until obtaining the molten state, 3 minutes of isothermal stage to ensure total chemical homogenization and about ten minutes for solidification and cooling down to ambient temperature.

The obtained ingots presented an ovoid shape. They were divided in four equal quarters, by sawing them with a metallographic cutter (Delta Abrasimet of Buehler). One of the four parts was divided in two parts and metallographically prepared to characterize the as-cast microstructure. Another one was kept for the oxidation test. This one was ground all around with 1200-SiC paper with smoothing of the edges. Thereafter it was washed and dried. The six prepared oxidation samples were placed in six alumina nacelles with only three contact points with these later ones. These nacelles were placed in a muffle furnace (HFL 16/17 model, Nabertherm, 12kW, 1700°C max).

After heating at 20K/min, the samples were maintained at 1400K (1127°C) during 20 hours, in air. After the isothermal oxidation stage the samples slowly cooled in the furnace off, until reaching about 650°C. They were then exited from the furnace (air-cooling). The oxidized samples were photographed, then prepared for the cross-sectional observations. The start of this preparation was to cathodically deposit gold all around to give the necessary electrical conductivity to the outer side of the oxides formed. Each gold-coated oxidized sample was then immersed in a Watt's bath heated at 50°C. It was then cathodically polarized to reduce the Ni^{2+} ions of the solution in metallic nickel. After about two hours at $0.016A/cm^2$, a sufficiently thick nickel shell was obtained all around the sample to ensure good protection of the external oxide scales during the subsequent cutting. The Ni-covered samples were cut in two parts which were thereafter embedded in cold resin (ESCIL), as the samples for the as-cast microstructure examinations. After about two hours in a 40°C stove, the resin was totally rigidified. The samples were then extracted from the mold. All the embedded samples, as-cast or oxidized, were ground with SiC papers from 240 to 1200-grit. After ultrasonic cleaning in water the samples were polished with 1µm hard particles sprayed on textile disk.

The mirror-like metallic top of the embedded samples were examined using a JEOL JSM-6010LA Scanning Electron Microscope (SEM), in Back Scattered Mode (BSE), with a 20kV acceleration voltage. The chemical compositions of the as-cast alloys were controlled by ×250 full frame measurements on three randomly chosen areas. Spot EDS analysis was also carried out in the matrix (center of dendrites) in three locations too, as well as on the seen particles. The same measurements were done again in the centers of the oxidized samples.

The oxides formed, externally or internally, were observed in BSE mode, and identified by spot EDS analysis. For each oxidized sample, a concentration profile was carried out from the scale/alloy interface, perpendicularly to this one, towards the not oxidation-affected part of the alloy.

RESULTS

Chemical compositions and as-cast microstructures of the six obtained alloys

The chemical compositions really obtained are displayed in Table 2. One can see that all contents are well respected. One can only notice that the chromium ones tend to be slightly too high for many alloy. The carbon content, which cannot be measured with the single available technique (SEM/EDS) because of its low atomic mass and its too low content in the alloy, can be expected as being well respected. Indeed, the applied protocol is exactly the same as many times used for similar alloys. In addition it is periodically controlled by spark spectrometry on samples of the same category, and each time validated. By looking to the density of the primary carbides obtained in the microstructures (Figure 1 and Figure 2), which is typical of many 0.4wt.%-containing alloys of the same family, the good respect of the targeted carbon content is confirmed.

The microstructures of the six alloys in their as-cast states are illustrated by SEM/BSE micrographs taken with two magnifications (general view and detailed view). All alloys are unsurprisingly dendritic, with three possible types of carbides. As suggested by the more or less high local concentrations, either in carbon and in chromium, or in carbon and titanium, the as-cast Co-poorest (i.e. Ni-richest) alloys contain almost exclusively chromium carbides (Figure 1). According to the spot analyses carried out on the coarsest carbides which were found, the atomic Cr/C ratio is close to 2 for the Ni0/5Co, Ni1/5Co (and seemingly Ni2/5Co too) alloys. This suggests that these chromium carbides are of the Cr_7C_3 stoichiometry, which is confirmed by the usual acicular shape of the carbide part of the interdendritic eutectic compound. In the Ni2/5Co alloy rare fine $Cr_{23}C_6$ are seemingly also present. They can be seen thanks to their paler tint in BSE mode, but they were too rare and fine to be identified as previously by qualitative EDS results. However, particles with a similar tint are a little more numerous in the Ni3/5Co, Ni4/5Co and Ni5/5Co alloys (Figure 2). Nevertheless they are really not the main carbide type present since TiC carbides are present in great quantity, especially in the two Co-richest alloys. In the Ni5/5Co alloy the interdendritic carbide network is almost exclusively made of TiC carbides, which are obviously of a eutectic nature. Indeed they are script-like carbides mixed with the periphery of the matrix dendrites. So, when the Co/Ni ratio rises from 0 to 1, the acicular-shaped eutectic Cr_7C_3 are progressively replaced by the Chinese script eutectic TiC carbides, with simultaneously appearance of more $Cr_{23}C_6$ carbides.

Results of oxidation

A quarter of each ingot, with preliminarily surface preparation, was subjected to a 20 hours exposure at 1400K in atmospheric air. Macrographs of the oxidized samples are presented in Figure 3 for the Co-poorest alloys and in Figure 4 for the Co-richest ones. All ingot quarter has obviously kept its oxide scale all around. However, one can see that spallation occurred, but this was rather limited. The metal is visible here and there, but the cumulative surface fraction of denuded alloy varies only between 95.8% to more than 99.5%, as this was measured by image analysis (tool of the Adobe Photoshop CS software). Furthermore, one can say that the surface fraction of denuded alloy tends to be a little greater for the Co-poorest alloys than for the Co-richest ones.

When observed on cross-sections, the three Co-poorest alloys are covered almost exclusively by Cr_2O_3 (Figure 5). This chromia scale is very compact for the Ni0/5Co and Ni1/5Co alloys but it becomes a little porous for the Ni2/5Co alloy. This obvious chromia-forming behavior demonstrated by the three Co-poorest alloys is lost, at least locally, for the three Co-richest alloys (Figure 6). Indeed, beside some areas covered by chromia, one finds here and there (Co,Ni)O or CoO oxides juxtaposed or superposed with chromia, with additionally presence of different spinel varieties ($CoCr_2O_4$, $TiCr_2O_4$). In all cases TiO_2 is also present: as an outer thin scale above chromia for the Co-poorest alloys, and as internal TiO_2 in the subsurface for all alloys. For the Co-richest alloys, oxidation becomes catastrophic in some location, with a penetration inwards the alloys. Generalized oxidation was obviously near to occur.

It was attempted to measure the thickness of the oxide scales on the cross-sections. Table 3 (first results column) displays the values of the averages and standard deviations. The oxide (chromia) is the lowest for the Co-poorest alloys, while the average values of thickness is the greatest for the Co-richest ones. One can note the great values of standard deviation resulting from the existence of many points of catastrophic oxidation for the later alloys.

Carbides, chromium carbides as well as titanium carbides, disappeared from the scale/alloy interface. This phenomenon, classical for alloys containing primary carbides, is here more extended for the Co-richest alloys, due to the obvious faster oxidation (Table 3, second results column). Nevertheless, because of the points of penetrating

oxidation, the local carbide-free depths can be lower, and taking them into account leads to lower average values and great values of standard deviation.

The carbide-free depths more or less correspond to the chromium concentration profiles (Figure 7 for the full scale profiles of the major elements Cr, Ni and Co of three of the six alloys), more precisely to the part with the greatest gradient (Table 4, second results column). The inner chromium depletion, with a Cr gradient a little lower, is included in the part of the alloy in which carbides are still here. Obviously, the disappearance of the interdendritic carbides induced little but existent difficulty for Cr diffusion towards the oxidation front. In this field, by noticing that the chromium gradients seem to be a little higher for the Co-richest alloys than for the Co-poorest ones, the diffusion of chromium may be less easy for the formers than for the latters. One can additionally note that the minimum Cr content in extreme surface was about the same (between 10 and 14 wt.%Cr) for all alloys. However the minimal chromium content seems to be maybe a little higher for the Co-poorest alloys than for the Co-richest alloys (Table 4, first results column).

Concerning titanium, depletions exist too for all alloys but the profile is often perturbed by the presence of internal titanium oxides or of TiC carbides. Ti seems having itself diffused towards the oxidation front and this explains the presence of titanium oxides and of spinels involving Ti as constituents of the external oxide scales.

DISCUSSION

As this was recently found concerning the dependence, on the nature of the base element, of the type of the primary carbides issued from solidification [8], the Ni0/5Co (Ni-based in fact) alloy contains almost exclusively chromium carbides while the Ni5/5Co (Co-based in fact) alloy contains here too almost exclusively TiC carbides (thanks to the atomic equivalence between Ti and C). These chromium carbides are Cr_7C_3, as is to say the high temperature type of chromium carbides usually found in {20 to 30wt.%Cr}-containing alloys in presence of about 0.5wt.%C. After solidification the cooling was probably too fast to allow the transformation of the high temperature Cr_7C_3 into the low temperature $Cr_{23}C_6$. These primary chromium carbides obviously solidified at the end of solidification, by forming a eutectic compound in the interdendritic spaces. This compound is composed of acicular carbides mixed with the periphery of the dendrites. The titanium carbides existing in the as-cast microstructure of the cobalt-based alloy (Ni5/5Co) are surely also eutectic carbides. They are themselves mixed with the periphery of the dendrites of matrix. Their morphology is different: Chinese script. A look to the bulk of the samples after their oxidation tests shows that the chromium carbides significantly evolved, more in term of morphology than in term of surface or volume fraction: they became rounder and more compact. This results in the loss of their matrix-imbricated character and probably of the reinforcement they may bring to the alloy at high temperature. In contrast, the TiC carbides kept their script-like morphology, even after 20 hours spent at the rather high temperature of 1400K (1127°C). Their presence and morphological stability let think to a good persistence of the strengthening effect at high temperature that they may bring to an alloy which is additionally already better than a nickel alloy in this field. If the Ni0/5Co cobalt-based alloy owns advantages to be mechanically resistant at high temperature, it is, in contrast, the worst in term of oxidation resistance: mainly cobalt oxides, spinels of different types, only a little chromia, numerous points of fast oxidation penetration, many voids in subsurface... The Ni0/5Co nickel-based alloys is the best in this field, with a protective chromia scale obviously of high quality (totally covering the sample, adherent to the metallic substrate, without too numerous and great porosities).

Between these two extreme alloys there are four other ones, with varying Co/(Ni+Co) ratios. The transition from chromium carbides to titanium carbides appears as being progressive, with transitorily low temperature $Cr_{23}C_6$ chromium carbides co-existing with TiC. Consequently the resistance of the carbides population against morphological evolution at high temperature increases, with favorable consequences for the sustainability of the high temperature strength. In the same time, the initially very good high temperature oxidation degenerates to become almost catastrophic. The transition from the degenerating good chromia-forming behavior to the start and generalization of the catastrophic oxidation, for the conditions in this work (atmospheric air, 20 hours, 1127°C), seems to occur between the Ni2/5Co alloy and the Ni3/5Co one, as is to say when the alloy series finishes to be nickel-based to start to be cobalt-based.

The participation of titanium in the general oxidation behavior was of several types. As earlier reported [9], this very reactive element was here internally oxidized in the subsurface of all alloys. This internal oxidation of titanium took place from its solid solution position in the case of the Co-poorest nickel-based alloys, as well as from the primary TiC carbides in the case of the Co-richest alloys. The formed titanium oxides are TiO_2 or spinel $TiCr_2O_4$, as suggested by the EDS spot analyses. In many cases an outer TiO_2 was also found above the chromia scale (mainly

for the nickel-based of this study). The limited spallation affected it first, with as result only isolated parts of TiO_2 along the unaffected adherent chromia scale. This layout is what is commonly reported for chromia-forming alloys containing titanium [10-14]. But titanium oxides were never really found mixed with the other oxides in the cases of the parts of samples catastrophically oxidized. So Ti, added initially to form strengthening carbides, took part to the oxidation process. By taking into account the rather small quantity of titanium oxides formed, for the chromia-forming nickel-based alloys as well as for the not well oxidation resistant cobalt-based ones, one may think that the presence of this element, sometimes claimed as being deleterious for the high temperature oxidation behavior [15], did not really influence the behaviors of the six alloys. The explanations of the differences of behavior of the well oxidation resistant Ni0/5Co to Ni/2/5Co alloys and the badly resistant Ni3/5Co to Ni5/5Co alloys is certainly more to be found in the intrinsic characteristics of the matrixes [16]. In the ones rich in nickel, chromium easily diffuses towards the oxidation front. It is furthermore helped by the presence of chromium carbides which may be considered as chromium reservoirs available in the interdendritic spaces. These reservoirs Cr deliver particularly efficiently since the interdendritic spaces act as fast diffusion paths for Cr. On the contrary, Cr diffusion is much slower in the cobalt-rich alloys: interdendritic spaces occupied by TiC rather than by chromium carbides, and more difficult diffusion through the matrixes rich in cobalt. One can be easily convinced by considering the evolution of the Cr concentration gradients and the chromium contents in extreme surface at the end of experiment (Table 4). But this can be also additionally illustrated numerically by giving the following values of chromium diffusion coefficients available in literature for Co-Cr and Ni-Cr model alloys (both at 1100°C): 2×10^{-11} cm²/s for Cr diffusion in Co-14Cr [17] and 26×10^{-11} cm²/s for Cr diffusion in Ni-25Cr [18].

CONCLUSION

Thus, it was here found again that the progressive substitution of nickel by cobalt favored the formation of the morphologically stable script-like TiC carbides at the expense of the less stable chromium carbides. Unfortunately this had also obviously as consequence to harm the alloy's behavior in oxidation at high temperature. It appeared that it was mainly the mean used for promoting the TiC presence, i.e. an increasing cobalt part, than the result (TiC rather than chromium carbides) which is responsible of this decrease in high temperature resistance. Fortunately it is still possible to improve the oxidation resistance, for example by enriching in chromium the TiC-containing alloys (rich in cobalt), either at the level of the whole composition (25 → 30wt.%Cr, or more) or locally (surface and subsurface enrichment in Cr, by pack cementation for example. This remains to be tested in future work.

References

1. M. J. Donachie, S. J. Donachie, *Superalloys: A Technical Guide (2nd Edition)*, Materials Park: ASM International, 2002.
2. P. T. B. Shaffer, *Plenum Press Handbooks of High Temperature Materials. Part 1: Materials Index*, New York: Plenum Press, 1964.
3. H. Matysiak, M. Zagorska et al, *Materials* **6(11)**, 5016 **(2013)**.
4. J. H. Chern Lin, S. J. Lo et al, *Journal of Oral Rehabilitation*, **22(5)**, 331 **(1995)**.
5. M. Gradzka-Dahlke, *Defect and Diffusion Forum* **297-301**, 1053 **(2010)**.
6. P. Berthod, E. Kretz et al, *Calphad* **56**, 41 **(2017)**.
7. M. Khair, P. Berthod, *Materials Science: An Indian Journal* **14(13)**, 102 **(2016)**.
8. L. Toubal, *Report of trainee period*, 1st year of Master of Chemistry, University of Lorraine, France **(2017)**.
9. K. A. Al-Hatab, M. A. Al-Bukhaiti et al, *Oxidation of Metals* **75(3-4)**, 209 **(2011)**.
10. P. Berthod, F. Allègre, et al, *Oxidation of Metals* **86**, 581 **(2016)**.
11. F. A. Perez-Gonzalez, J. H. Ramirez-Ramirez, et al, *Corrosion Engineering, Science and Technology* **51(7)**, 513 **(2016)**.
12. A. Jalowicka, W. Nowak, et al, *Oxidation of Metals* **83(3-4)**, 393 **(2015)**.
13. F. A. Perez-Gonzalez, N. F. Garz-Montes-de Oca, et al, *Oxidation of Metals*, **82(3-4)**, 145 **(2014)**.
14. J. Litz, A. Rahmel, et al, *Oxidation of Metals* **32(3-4)**, 167 **(1989)**.
15. S. W. Yang, *Oxidation of Metals*, **15(5-6)**, 375 **(1981)**.
16. D. Young, *High Temperature Oxidation and Corrosion of Metals*, Amsterdam: Elsevier Corrosion Series, 2008.
17. J. W. Weeton, *Diffusion of chromium in alpha cobalt-chromium solid solutions*, Report 1023 of the National Advisory Committee for Aeronautics (**1951**).
18. P. Berthod, E. Conrath, *Materials Chemistry and Physics* **165**, 79 **(2015)**.

TABLE 1. Targeted compositions for the six alloys of the study (weight contents).

Alloys	Ni	Co	Cr	Ti	C
"Ni0/5Co"	Bal.	0	25	1.6	0.4
"Ni1/5Co"	Bal.	14.6	25	1.6	0.4
"Ni2/5Co"	Bal.	29.2	25	1.6	0.4
"Ni3/5Co"	29.2	Bal.	25	1.6	0.4
"Ni4/5Co"	14.6	Bal.	25	1.6	0.4
"Ni5/5Co"	0	Bal.	25	1.6	0.4

TABLE 2. Obtained chemical compositions (in wt.%); average and standard deviation of three full-frame SEM/EDS measurements carried out at the ×250 magnification)

Alloys	Ni	Co	Cr	Ti	C
"Ni0/5Co"	Bal.	/	25.4 ±0.2	1.6 ±0.1	"0.4"*
"Ni1/5Co"	Bal.	14.5 ±0.1	25.6 ±0.2	1.6 ±0.1	"0.4"*
"Ni2/5Co"	Bal.	29.1 ±0.3	25.3 ±0.2	1.5 ±0.1	"0.4"*
"Ni3/5Co"	29.4 ±0.1	Bal.	25.3 ±0.3	1.6 ±0.1	"0.4"*
"Ni4/5Co"	14.8 ±0.1	Bal.	25.6 ±0.3	1.7 ±0.1	"0.4"*
"Ni5/5Co"	/	Bal.	25.7 ±0.1	1.6 ±0.1	"0.4"*

*: carbon contents not controlled by EDS but assumed to be well respected according to the practical knowledge for the elaboration protocol for many alloys before, and confirmed by the obtained density of carbides

TABLE 3. Obtained chemical compositions (in wt.%); average and standard deviation of three full-frame SEM/EDS measurements carried out at the ×250 magnification)

Alloys	Oxide scale thickness (µm)	Carbides-free zone depth (µm)
"Ni0/5Co"	18.1 ±0.5	26.1 ±1.0
"Ni1/5Co"	21.1 ±1.0	37.8 ±3.5
"Ni2/5Co"	16.1 ±2.6	28.9 ±3.5
"Ni3/5Co"	3-10µm *	45.6 ±4.2
"Ni4/5Co"	23.9 ±16.8	35.6 ±9.5
"Ni5/5Co"	34.4 ±21.5	27.8 ±4.8

*: probably minimized because one suspects that an external part of the scale was lost by spallation

TABLE 4. Average and standard deviation for the chromium content in alloy close to the external scale/alloy interface (three measurements); assessment of the chromium gradients from the concentration profiles

Alloys	Chromium content in extreme surface (wt.%)	Cr concentration gradients from the scale/alloy interface (wt.%/µm)
"Ni0/5Co"	13.6 ±0.6	0.15 over ≈ 65µm
"Ni1/5Co"	13.4 ±0.4	0.30 over ≈ 35µm, and 0.08 deeper
"Ni2/5Co"	12.1 ±0.9	0.33 over ≈ 40µm, and 0.12 deeper**
"Ni3/5Co"	12.5 ±0.3	0.23 over ≈ 45µm, and 0.11 deeper
"Ni4/5Co"	10.3 ±4.1*	0.23 over ≈ 50µm
"Ni5/5Co"	11.0 ±1.6	0.25 over ≈ 50µm

*: great variations (e.g. between 5.7 and 13.5wt.%Cr); **: illustration in Figure 7

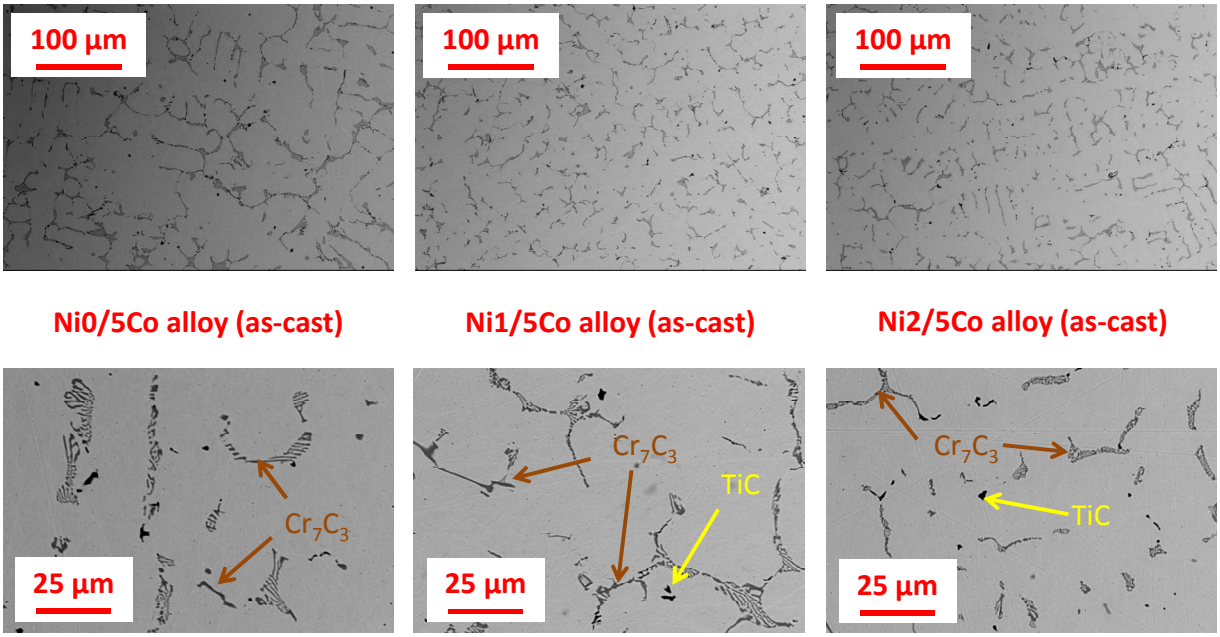

FIGURE 1. As-cast microstructure of the three Co-poorest alloys (SEM/BSE; top: ×250; bottom: ×1000)

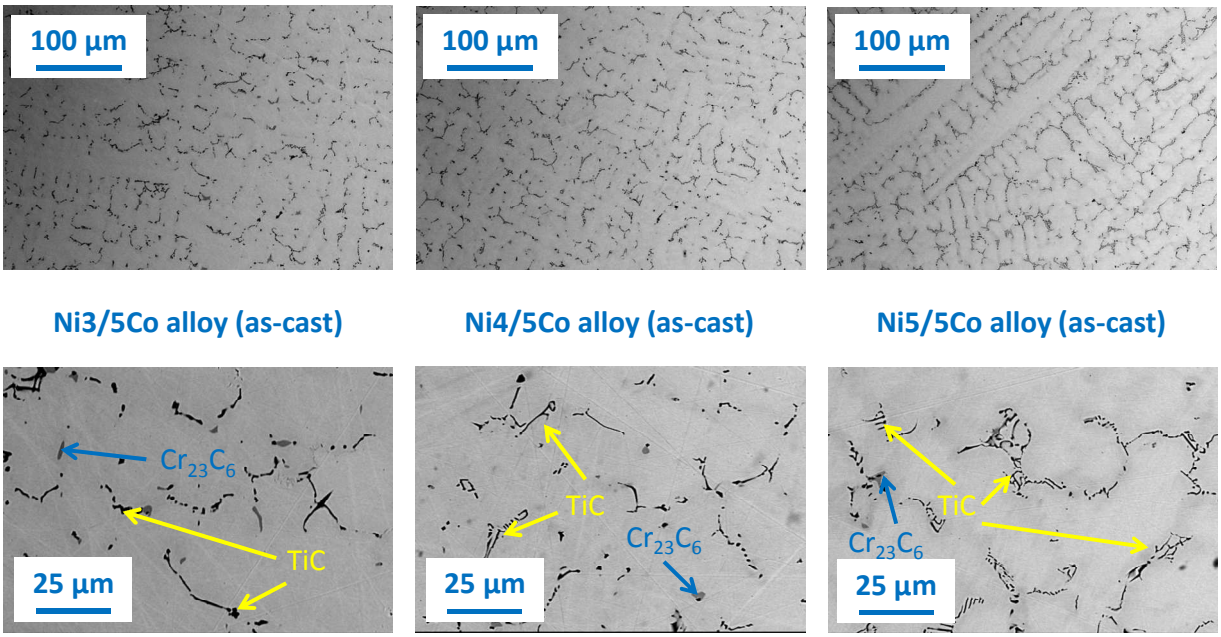

FIGURE 2. As-cast microstructure of the three Co-richest alloys (SEM/BSE; top: ×250; bottom: ×1000)

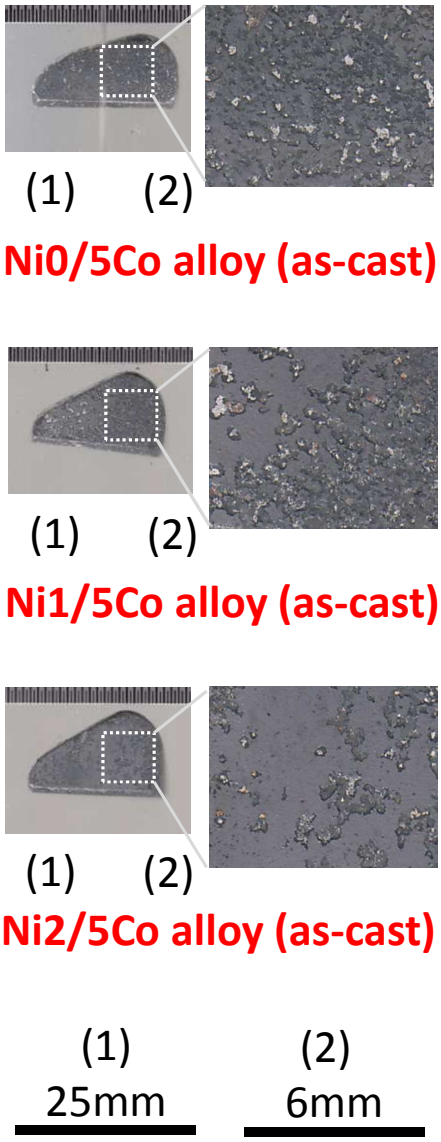

FIGURE 3. Macrographs illustrating the oxidized state of the three Co-poorest samples

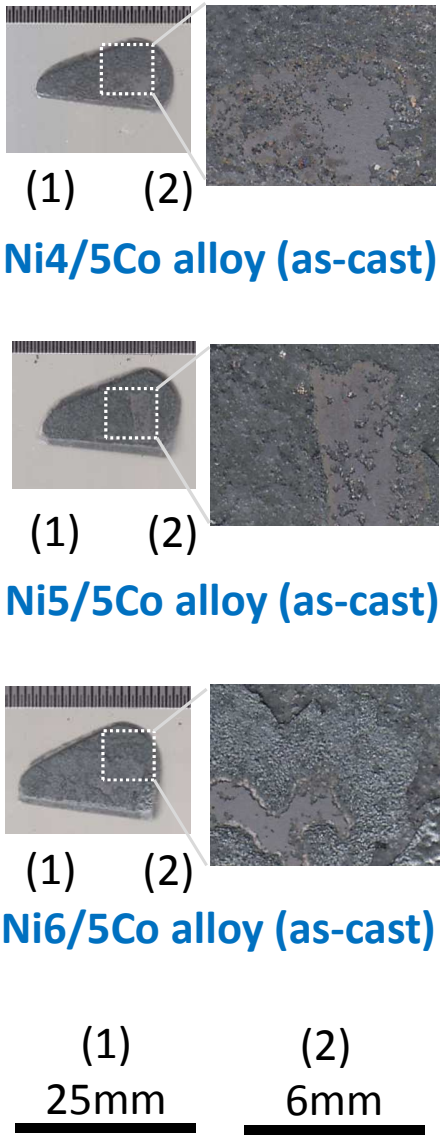

FIGURE 4. Macrographs illustrating the oxidized state of the three Co-richest samples

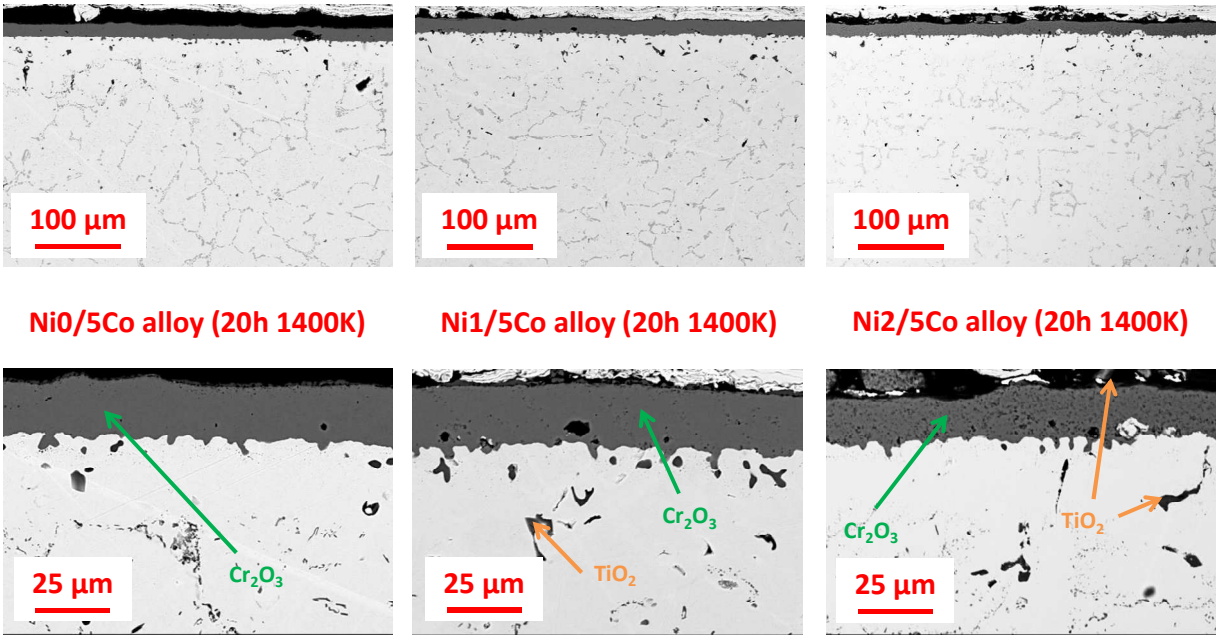

FIGURE 5. Cross-sectional examination of the oxide scales and subsurfaces of the three Co-poorest alloys (SEM/BSE; top: ×250; bottom: ×1000).

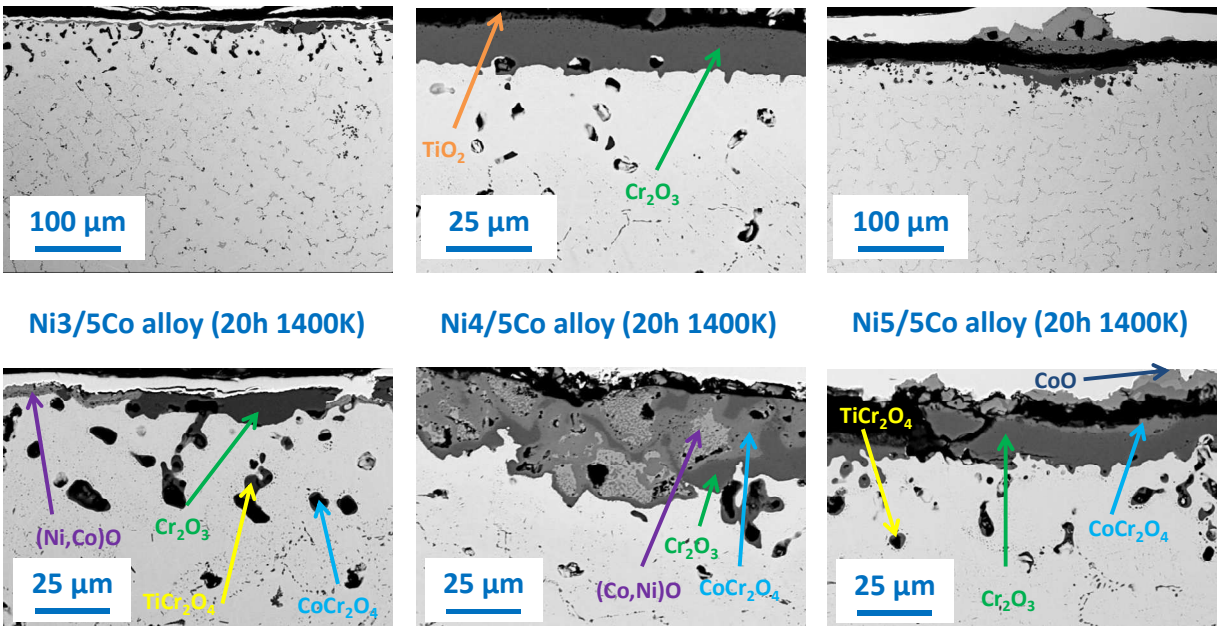

FIGURE 6 Cross-sectional examination of the oxide scales and subsurfaces of the three Co-richest alloys (SEM/BSE; top: ×250; bottom: ×1000).

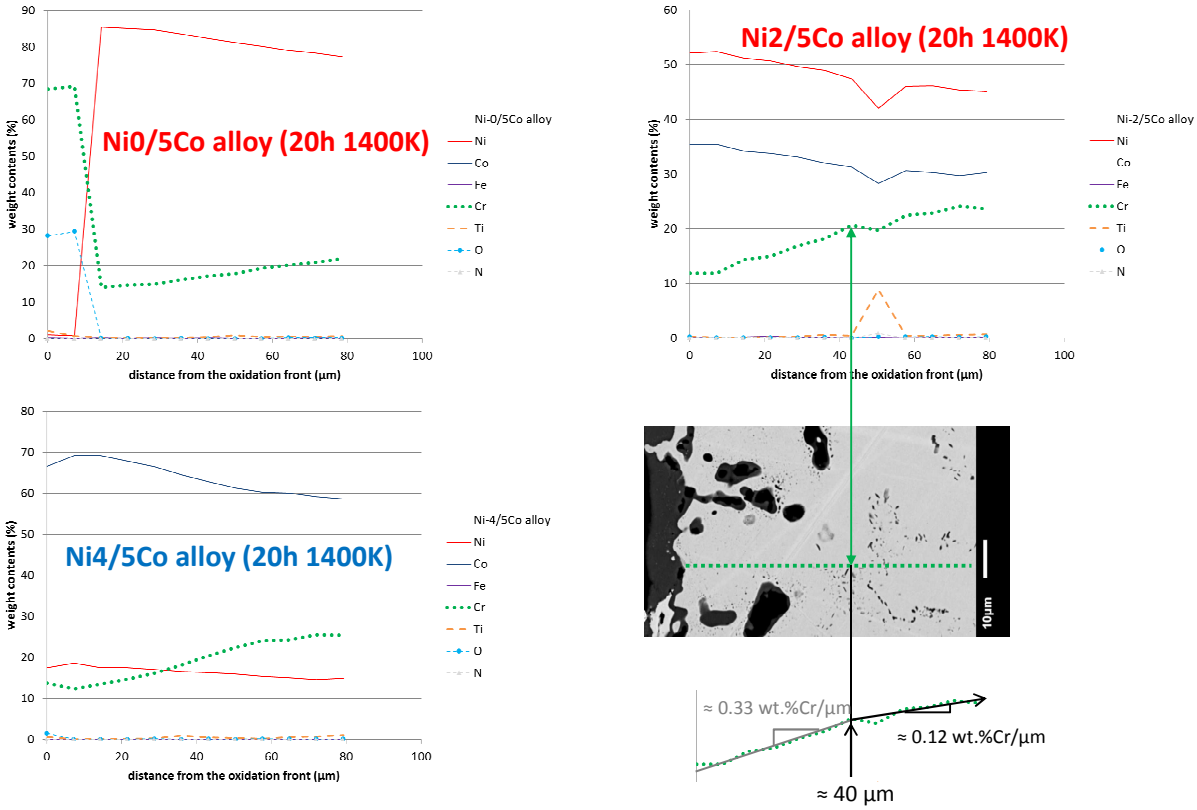

FIGURE 7. Concentration profiles in the subsurfaces of three of the six alloys (SEM/EDS); full scale.

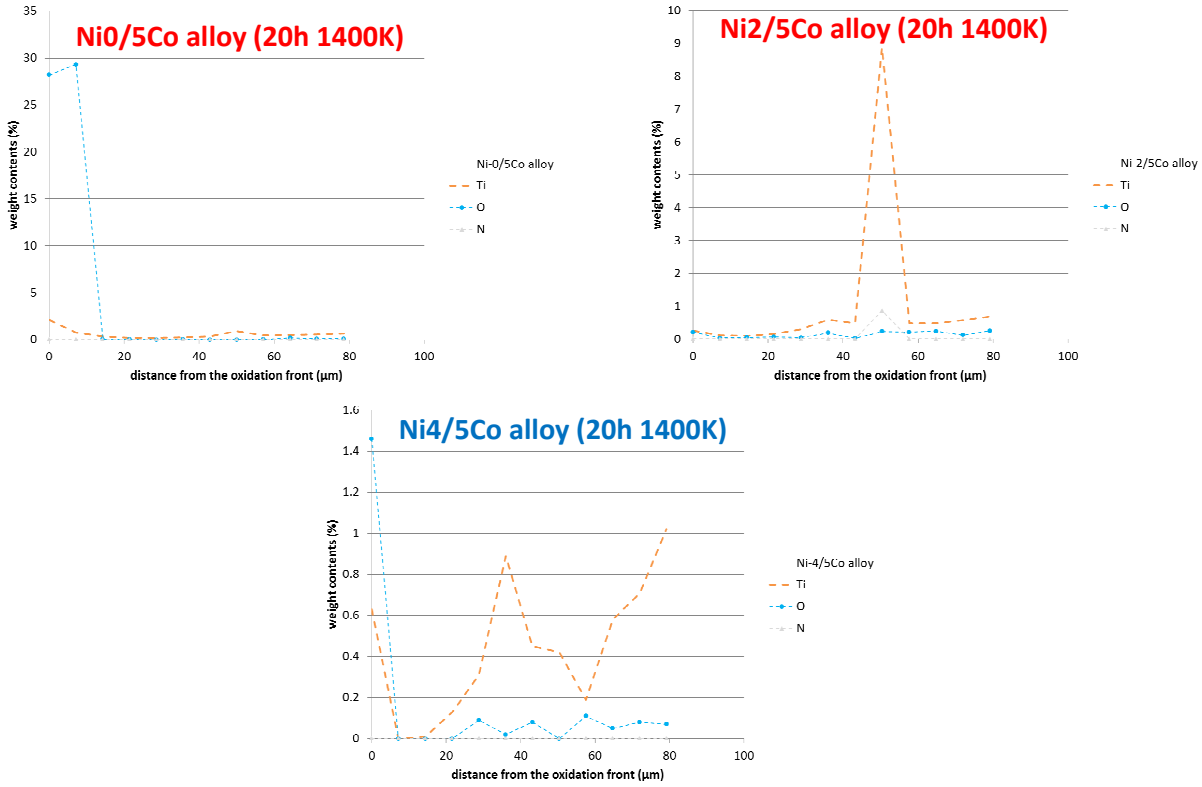

FIGURE 8. Concentration profiles in the subsurfaces of three of the six alloys (SEM/EDS); enlarged view.